Generalized master equations for non-Poisson dynamics on networks

Till Hoffmann
Department of Physics, University of Oxford, Oxford, United Kingdom

Mason A. Porter
Oxford Centre for Industrial and Applied Mathematics, Mathematical Institute, University of Oxford, Oxford, OX1 3LB, United Kingdom and CABDyN Complexity Centre, University of Oxford, Oxford OX1 1HP, United Kingdom

Renaud Lambiotte*
Naxys, University of Namur, B-5000 Namur, Belgium and
Department of Mathematics, University of Namur, B-5000 Namur, Belgium

(Received 14 December 2011; revised manuscript received 4 August 2012; published 8 October 2012)

The traditional way of studying temporal networks is to aggregate the dynamics of the edges to create a static weighted network. This implicitly assumes that the edges are governed by Poisson processes, which is not typically the case in empirical temporal networks. Accordingly, we examine the effects of non-Poisson inter-event statistics on the dynamics of edges, and we apply the concept of a generalized master equation to the study of continuous-time random walks on networks. We show that this equation reduces to the standard rate equations when the underlying process is Poissonian and that its stationary solution is determined by an effective transition matrix whose leading eigenvector is easy to calculate. We conduct numerical simulations and also derive analytical results for the stationary solution under the assumption that all edges have the same waiting-time distribution. We discuss the implications of our work for dynamical processes on temporal networks and for the construction of network diagnostics that take into account their nontrivial stochastic nature.

DOI: 10.1103/PhysRevE.86.046102 PACS number(s): 89.75.Fb, 89.90.+n

I. INTRODUCTION

Over the past two decades, myriad papers have illustrated that understanding complex systems composed of large numbers of interacting entities can be improved considerably by adopting a network-science perspective [1]. In particular, the influence of network architecture on dynamical processes such as random walks, biological and social epidemics, and opinion formation is now well appreciated (and somewhat better understood than it used to be) [2]. The effects of network structure on dynamics on networks have been investigated using a variety of techniques, including mean-field theories and pair approximations, spectral methods, and numerical simulations [3].

In the study of dynamics on networks, there has been intense focus on network structure—that is, the arrangement of edges and their associated weights—but the effects of the temporal patterns of edges remains very poorly understood [4]. In a realistic setting, many networks are not static, as edges and nodes can appear and disappear, and this has a strong effect on spreading processes [5–12]. Most studies of networks tend to overlook such temporal patterns by assuming a time-independent set of nodes and assigning a single scalar to represent a weighted edge A_{ij} between each pair of nodes i and j. This scalar is supposed to represent some sort of aggregate importance of the connection between i and j, and it is often understood as a rate in the case of continuous-time processes [13]. From such a Poisson perspective, the probability that an edge appears between two nodes i and j in a time interval of length dt is given by $dt/\langle\tau_{ij}\rangle$, where $\langle\tau_{ij}\rangle \equiv 1/A_{ij}$ (and $\tau_{ij} = +\infty$ if i and j are not connected by an edge) is the mean inter-event time and the time τ between two consecutive events obeys an exponential distribution with mean $\langle\tau\rangle$.

This Poisson assumption facilitates theoretical analysis, provides intuitive results, and is reasonably accurate for a variety of systems in which the rate at which events take place does not depend on their histories. However, numerous systems (especially socioeconomic ones) exhibit non-Poisson temporal statistics due to their nonstationarity or their non-Markovian nature. Observations in financial markets [14]; e-mail [15–18], postal [19], and online [20,21] communication networks; face-to-face contacts [22]; movie rentals [23]; and many other situations have illustrated that the time intervals between isolated actions performed by an individual or between isolated interactions for a pair of individuals deviates significantly from a Poisson process. Such behavior has important implications for the spread of epidemics [24], social influence [25], and more.

Two perspectives have been used to attempt to go beyond the unrealistic Poisson assumption. First, one can perform simulations on temporal graphs for which a time series of the presence versus absence of edges is deduced directly from empirical observations [9,10]. However, such a computational approach has a significant drawback: It relies entirely on simulations and/or algorithms to produce, for example, time-randomized versions of the original data, and it is thus unable to improve underlying theoretical understanding or build predictive models. Second, one can study problems in a more abstract manner by developing spreading models that incorporate realistic temporal statistics. Such models can then be studied either mathematically or using numerical simulations [11,13]. In this second approach, an underlying network is treated as a fluctuating entity. One typically assumes

*renaud.lambiotte@fundp.ac.be

that it is driven by a stationary stochastic process, which allows exhaustive computational experimentation through the analysis of ensembles of realizations and by tuning structural and temporal parameters. This modeling perspective also lends itself to mathematical analysis [26,27], though most research on it thus far has been computational in nature.

In this paper, we take the second approach and argue for the development of a mathematical framework to explore the effect of non-Poisson inter-event statistics on dynamics. To do so, we apply the concept of a generalized master equation [28], which is traditionally defined on networks with regular structures (i.e., on regular lattices) to the study of continuous-time random walks on networks. Generalized master equations lie at the heart of the theory for anomalous diffusion and have applications ranging from ecology [29] to transport in materials [30]. Our choice regarding what dynamics to consider is motivated by the importance of random walks as a way to understand how network structure affects dynamics and to uncover prominent structural features from networks.

The rest of this paper is organized as follows. We first introduce the process and derive its generalized master equation in both ordinary space and Laplace space. After checking that the equation reduces to standard rate equations when the underlying process satisfies Poisson statistics, we focus on its stationary solution and show that it is determined by an effective transition matrix whose leading eigenvector can be calculated rapidly even in very large networks. After validating theoretical predictions by using numerical simulations, we discuss the implications of our work in terms of dynamical processes on time-dependent networks and for the construction of network diagnostics that take into account their nontrivial stochastic nature.

II. GENERALIZED MASTER EQUATION

In this section, we derive a generalized master equation for continuous-time random walks with arbitrary waiting-time statistics.

A. Beyond static weights on edges

Consider the N-node directed graph $\mathcal{G}$ in Fig. 1. To avoid unnecessary complications, we assume for this discussion that $\mathcal{G}$ is strongly connected (so one can reach any node starting from any other node). A network is typically represented using an adjacency matrix A whose elements A_{ij} indicate the connection strength between each pair of nodes i and j.

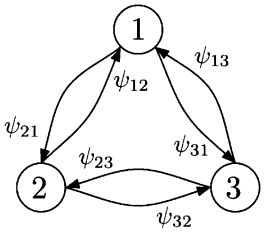

FIG. 1. A directed graph with $N = 3$ nodes and no self-loops. The waiting-time distribution $\psi_{ij}(t)$ characterizes the appearances of an edge from j to i.

For an unweighted network, A_{ij} can take either the value 1 (if there is an edge) or the value 0 (if there is not an edge). For a weighted network, A_{ij} can take an arbitrary real value (which is assumed to be non-negative in most studies), and a value of 0 again indicates the absence of an edge.

Whether considering a weighted or an unweighted network, one typically aggregates networks evolving over a certain time interval and thus ignores the temporal pattern of edges, which can be of critical importance in empirical situations [4]. We propose instead to assign to each edge an inter-event time distribution that determines when a edge is accessible for transport. The dynamics of a network are thus characterized by an $N \times N$ matrix $\psi(t)$ of smooth, piecewise continuous waiting-time distributions (WTDs) $\psi_{ij}(t)$ that determine the appearances of an edge emanating from node j and arriving at node i. We also assume that the edges remain present for infinitesimally small times, which implies that the network is empty (and thus that the entries of the adjacency matrix are 0) except at random instantaneous times determined by $\psi(t)$, when a single edge is present. From now on, we use the following terminology: $\mathcal{G}$ is called the underlying graph (i.e., this graph determines which edges are allowed and which are not) and $\psi_{ij}(t)$ determines a dynamical graph, in which edges appear randomly according to the assigned waiting times. We use this random process to model the transitions of a random walker moving on the graph. By construction, a walker located at a node j remains on it until an edge leaving j toward some node i appears. When such an event occurs, the walker jumps to i without delay (i.e., there is no waiting time) and waits until an edge leaving i appears.

There are several ways that one can set up the WTDs $\psi_{ij}(t)$. We consider the case in which a WTD corresponds to the probability for an edge to occur between time t and $t + dt$ after the random walker arrives on node j in the previous jump. In other words, all edges leaving j have their clocks reinitialized when a walker arrives on it.[1] It follows from the definition of a WTD that

$$\int_0^\infty \psi_{ij}(t) = 1.$$

The probability that an edge appears between j and i before time t is

$$\int_0^t \psi_{ij}(t')dt',$$

and the probability that it does not appear before time t is therefore

$$\chi_{ij}(t) \equiv 1 - \int_0^t \psi_{ij}(t')dt'. \tag{1}$$

If a transition from j to i is not allowed, then the corresponding element $\psi_{ij}(t)$ is equal to 0 for all times. Additionally, we assume for simplicity that the underlying network $\mathcal{G}$ has no self-loops.

It is important to distinguish between the WTD $\psi_{ij}(t)$ of a process that might lead to a step along an edge and the

[1] Another possibility is that edges can appear incident to nodes according to independent processes.

probability distribution $T_{ij}(t)$ for actually making a step to i. This distinction is necessary because all of the processes on a node are assumed to be independent of one another, but the probability to make a step depends on all of the processes. As an illustration, consider a walker on a node j with only one outgoing edge to i. The probability distribution function (PDF) to make a step to i a time t after having arrived on j is then

$$T_{ij}(t) = \psi_{ij}(t).$$

However, if there exists another edge leaving j (e.g., an edge to node k), then the PDF to make a transition to i is modified, as a step to i occurs only if the edge to i appears before the one going to k. In this situation,

$$T_{ij}(t) = \psi_{ij}(t)\chi_{kj}(t).$$

In general, the PDF to make a step from j to i accounting for all other processes on j is

$$\begin{aligned} T_{ij}(t) &= \psi_{ij}(t)\prod_{k\neq i}\chi_{kj}(t) \\ &= \psi_{ij}(t)\prod_{k\neq i}\left(1-\int_0^t \psi_{kj}(t')dt'\right). \end{aligned} \tag{2}$$

Equation (2) emphasizes the importance of the temporal ordering of the edges in a diffusive process. It can also be written as

$$T_{ij}(t) = -\frac{d\chi_{ij}(t)}{dt}\prod_{k\neq i}\chi_{kj}(t), \tag{3}$$

as $\chi'_{ij}(t) = -\psi_{ij}(t)$. An extreme scenario occurs when $\psi_{ij} = \delta(t-t_{ij})$ and $\psi_{kj} = \delta(t-t_{kj})$ for $t_{ij} > t_{kj}$. In this case, $T_{ij}(t) = 0$, so a walker located on j never takes the edge to i even if this edge appears very frequently as a function of time.

B. Generalized Montroll-Weiss equation

We now focus on the trajectories of a random walker exploring a temporal, stochastic network. We closely follow the standard derivation of the Montroll-Weiss (MW) equation [28] and generalize it to an arbitrary N-node network of transitions. The probability $n_i(t)$ to find a walker on node i at time t is the integral over all probabilities $q_i(t')$ of having arrived on i at time $t' \leqslant t$, weighted by the probability $\phi_i(t-t')$ of not having left the node since then:

$$n_i(t) = \int_0^t \phi_i(t-t')q_i(t')dt'. \tag{4}$$

We take the Laplace transform $\hat{n}_i(s) \equiv \mathcal{L}\{n_i(t)\} = \int_0^\infty n_i(t)e^{-st}dt$ to exploit the fact that the convolution reduces to a product in Laplace space [31]:

$$\hat{n}_i(s) = \hat{\phi}_i(s)\hat{q}_i(s). \tag{5}$$

We obtain the quantity $\hat{\phi}_i(s)$ from the PDF as follows. Making a step from node i to any other node gives

$$T_i(t) = \sum_{j=1}^{N} T_{ji}(t). \tag{6}$$

(Note that $T_{ii} = 0$ because there are no self-loops.) The PDF to remain immobile on node i for a time t is thus

$$\phi_i = 1 - \int_0^t T_i(t')dt'. \tag{7}$$

Taking the Laplace transform of equation (7) yields

$$\hat{\phi}_i(s) = \frac{1}{s}(1-\hat{T}_i(s)). \tag{8}$$

The quantity $\hat{q}_i(s)$ is the Laplace transform of the PDF $q_i(t)$ to arrive on node i exactly at time t. One calculates it by accounting for all k-step processes that can lead to such an event [32]:

$$q_i(t) \equiv \sum_{k=0}^{\infty} q_i^{(k)}(t),$$

where $q_i^{(k)}(t)$ represents the probability of arriving on node i at time t in exactly k steps. Note that the PDF at node i is related to that at node j by the recursion relation

$$q_i^{(k+1)}(t) = \int_0^t d\tau \sum_j T_{ij}(t-\tau)q_j^{(k)}(\tau). \tag{9}$$

In other words, the probability of arriving on node i in $k+1$ steps is the probability of arriving at any other node j in k steps weighted by the probability of making a step $j \to i$ at the required time.

Upon taking a Laplace transform, equation (9) becomes

$$\hat{q}_i^{(k+1)}(s) = \sum_j \hat{T}_{ij}(s)\hat{q}_j^{(k)}(s).$$

Summing over all k and adding $\hat{q}_i^{(0)}(s)$ yields

$$\hat{q}_i^{(0)}(s) + \sum_{k=0}^{\infty}\hat{q}_i^{(k+1)}(s) = \sum_j \hat{T}_{ij}(s)\sum_{k=0}^{\infty}\hat{q}_j^{(k)}(s) + \hat{q}_i^{(0)}(s),$$

which can also be written in terms of matrices and vectors:

$$\hat{q}(s) = \hat{T}(s)\hat{q}(s) + \hat{q}^{(0)}(s).$$

Noting that $q^{(0)}(t) = n(0)\delta(t)$, we see that the last term is simply $n(0)$, which leads to the following solution in Laplace space:

$$\hat{q}(s) = (I - \hat{T}(s))^{-1}n(0). \tag{10}$$

We insert the expression (8) for $\hat{\phi}_i(s)$ and the expression (10) for $\hat{q}_i(s)$ into the equation for the walker density (5) to obtain a generalization of the MW equation [28] that applies to arbitrary network structures:

$$\begin{aligned} \hat{n}_i(s) &= \frac{1}{s}(1-\hat{T}_i(s))\sum_k (I-\hat{T}(s))^{-1}_{ik}n_k(0) \\ &= \sum_{jk}\frac{1}{s}(I_{ij} - \hat{T}_i(s)\delta_{ij})(I-\hat{T}(s))^{-1}_{jk}n_k(0). \end{aligned} \tag{11}$$

In terms of vectors and matrices, this is written

$$\hat{n}(s) = \frac{1}{s}(I - \hat{D}_T(s))(I-\hat{T}(s))^{-1}n(0), \tag{12}$$

where the diagonal matrix $\hat{D}_T$ has coordinates

$$(\hat{D}_T)_{ij}(s) = \hat{T}_i(s)\delta_{ij}. \tag{13}$$

Equation (12) is a formal solution in Laplace space for the density of a random walk whose dynamics are governed by the WTDs $\psi_{ij}(t)$. However, taking the inverse Laplace transform to obtain the random-walker density as a function of time does not in general yield closed-form solutions.

C. Integrodifferential master equation

The generalized master equation (12) is an integrodifferential equation that describes the evolution of the system in the time domain. In principle, it can be solved numerically to obtain the random-walker density as a function of time. To do this, we need to use the property $\mathcal{L}[\frac{dn}{dt}] = s\hat{n}(s) - n(0)$ of the Laplace transform, which holds provided that the Laplace transform of $n(t)$ and its derivative exist. As we show later, the walker density remains properly normalized.

We define the matrices $A \equiv I - \hat{D}_T(s)$ and $B \equiv I - \hat{T}(s)$. We then insert $\hat{n}(s)$ from the generalized Montroll-Weiss equation (12) to obtain

$$\begin{aligned}\mathcal{L}\left[\frac{dn}{dt}\right] &= s\hat{n}(s) - n(0)\\ &= (AB^{-1} - I)(sBA^{-1})\left(\frac{1}{s}AB^{-1}n(0)\right)\\ &= (A - B)sA^{-1}\hat{n}(s).\end{aligned}$$

Using the definitions for A and B and simplifying yields

$$\begin{aligned}\mathcal{L}\left[\frac{dn}{dt}\right] &= (\hat{T}(s) - \hat{D}_T(s))\frac{s}{I - \hat{D}_T(s)}\hat{n}(s)\\ &= \left(\hat{T}(s)\hat{D}_T^{-1}(s) - I\right)\frac{s\hat{D}_T(s)}{I - \hat{D}_T(s)}\hat{n}(s)\\ &= \left(\hat{T}(s)\hat{D}_T^{-1}(s) - I\right)\hat{K}(s)\hat{n}(s),\end{aligned} \tag{14}$$

where we have defined the Laplace transform of the *memory kernel* K as

$$\hat{K}(s) \equiv \frac{s\hat{D}_T(s)}{I - \hat{D}_T(s)}. \tag{15}$$

The memory kernel characterizes the amount of memory in the dynamics [33]. The memory kernel $K(t)$ is usually a function spanning over a nonvanishing time period. A notable exception is a Poisson process, for which $K(t) = \delta(t)$. The entries of $\hat{D}_T(s)$ are strictly smaller than 1 for all finite s because $\hat{T}_j(s) = \int_0^\infty e^{-st}T_j(t)dt < \int_0^\infty T_j(t)dt = 1$ (as we show in Sec. II E). Hence, the term $I - \hat{D}_T(s)$ is always invertible.

Taking the inverse Laplace transform of (14) leads to the generalized master equation

$$\frac{dn}{dt} = \left(T(t) * \mathcal{L}^{-1}\left\{\hat{D}_T^{-1}(s)\right\} - \delta(t)\right) * K(t) * n(t), \tag{16}$$

where $\mathcal{L}^{-1}$ denotes the inverse Laplace transform and $f * g = \int_0^t d\tau f(t-\tau)g(\tau)$ denotes convolution with respect to time. Unfortunately, mathematical analysis of Eq. (16) is difficult. However, as we exploit later, it is often significantly easier to analyze its Laplace-space equivalent (12).

Note that $\hat{D}_T(s)$ can in principle be singular, but considering $\hat{D}_T^{-1}(s)\hat{K}(s) = \frac{s}{I-\hat{D}_T(s)}$ as a single term resolves this issue.

D. Conservation of probability

The total number of random walkers is a conserved quantity, so $\frac{d}{dt}\sum_i n_i(t) = 0$. It is not easy to verify this directly in the time domain using Eq. (16). Thankfully, it is sufficient to show that the Laplace transform of the rate of change of the number of walkers vanishes because $\mathcal{L}^{-1}\{0\} = 0$. The inverse Laplace transform is unique except for null functions, which satisfy $\int_0^a \mathcal{N}(t)\,dt = 0$ for all $a > 0$. By assuming that the WTDs are piecewise continuous, we exclude null functions and the inverse Laplace transform is guaranteed to be unique [31,34].

Equation (14) gives the rate of change of the total walker density in Laplace space:

$$\begin{aligned}&\sum_{ij}\left[\left(\hat{T}(s)\hat{D}_T^{-1}(s) - I\right)\right]_{ij}[\hat{K}(s)\hat{n}(s)]_j\\ &\quad= \sum_{ikj}\left(\hat{T}_{ik}(s)\left[\hat{D}_T^{-1}(s)\right]_{kj} - \delta_{ik}\delta_{kj}\right)[\hat{K}(s)\hat{n}(s)]_j\\ &\quad= \sum_{ikj}\left(\hat{T}_{ik}(s)\frac{1}{\hat{T}_k(s)} - \delta_{ik}\right)\delta_{kj}[\hat{K}(s)\hat{n}(s)]_j\\ &\quad= \sum_{k}\left(\frac{1}{\hat{T}_k(s)}\left[\sum_i \hat{T}_{ik}(s)\right] - 1\right)[\hat{K}(s)\hat{n}(s)]_k = 0,\end{aligned}$$

which confirms that the rate of change of the total walker density vanishes.

E. Making steps in infinite time

In this paper, we have assumed that the underlying graph $\mathcal{G}$ of potential edges is strongly connected, which implies that a transition from j to some other node is guaranteed to occur eventually if one allows infinite time. We thus expect that $\int_0^\infty T_j(t)dt = 1$, as $T_j(t)$ is the PDF to make any transition from j. We use Eqs. (3) and (6) to obtain

$$\begin{aligned}T_j(t) = \sum_{i=1}^N T_{ij}(t) &= -\sum_{i=1}^N\left(\frac{d\chi_{ij}(t)}{dt}\times\prod_{k\neq i}\chi_{kj}(t)\right)\\ &= -\frac{d}{dt}\left(\prod_{i=1}^N\chi_{ij}(t)\right).\end{aligned}$$

Integrating over the entire time domain yields

$$\begin{aligned}\int_0^\infty T_j(t)dt &= -\int_0^\infty dt\frac{d}{dt}\left(\prod_{i=1}^N\chi_{ij}(t)\right)\\ &= -\left(\prod_{i=1}^N\chi_{ij}(t)\right)\Bigg|_{t=0}^\infty = 1,\end{aligned}$$

because $\chi_{ij}(0) = 1$ and $\chi_{ij}(\infty) = 0$ when the edge $j \to i$ exists in the underlying graph. (Otherwise, $\chi_{ij}(0) = 1$ and $\chi_{ij}(\infty) = 1$.)

F. Poisson limit

Assume that edge dynamics are Poisson processes and that the WTDs are exponential distributions [35] with a characteristic rate λ_{ij} for the transition $j \to i$. That is,

$$\psi_{ij}(t) = \lambda_{ij}e^{-\lambda_{ij}t}. \tag{17}$$

Equations (2) and (6) then imply that

$$T_{ij}(t) = \lambda_{ij} e^{-\lambda_{ij} t} \prod_{l \neq i} \left(1 - \int_0^t \lambda_{lj} e^{-\lambda_{lj} t'} dt' \right)$$
$$= \lambda_{ij} e^{-\lambda_{ij} t} \prod_{l \neq i} e^{-\lambda_{lj} t} = \lambda_{ij} e^{-\Lambda_j t}, \quad (18)$$

so

$$T_j(t) = \sum_{i=1}^{N} \lambda_{ij} e^{-\Lambda_j t} = \Lambda_j e^{-\Lambda_j t},$$

where the aggregate transition rate from j is $\Lambda_j \equiv \sum_{i=1}^{N} \lambda_{ij}$. The Laplace transform of $T_j(t)$ is

$$\hat{T}_j(s) = \frac{\Lambda_j}{\Lambda_j + s}.$$

Equation (13) then becomes

$$[\hat{D}_T(s)]_{ij} = \frac{\Lambda_j}{\Lambda_j + s} \delta_{ij},$$

which in turn yields

$$\left[\hat{D}_T^{-1}(s)\right]_{ij} = \left(1 + \frac{s}{\Lambda_j} \right) \delta_{ij}. \quad (19)$$

Equation (15) becomes

$$\hat{K}_{ij}(s) = \frac{s \frac{\Lambda_j}{\Lambda_j + s}}{1 - \frac{\Lambda_j}{\Lambda_j + s}} \delta_{ij} = \frac{s \Lambda_j}{\Lambda_j + s - \Lambda_j} \delta_{ij} = \Lambda_j \delta_{ij}. \quad (20)$$

Taking the inverse Laplace transform of Eq. (19) then yields

$$\mathcal{L}^{-1}\left\{\left[\hat{D}_T^{-1}(s)\right]_{ij}\right\} = \left(\delta(t) + \frac{\delta'(t)}{\Lambda_j} \right) \delta_{ij}, \quad (21)$$

and taking the inverse Laplace transform of Eq. (20) gives

$$K_{ij}(t) = \Lambda_j \delta(t) \delta_{ij}. \quad (22)$$

We insert Eqs. (18), (21), and (22) into the generalized master equation (16) and use the properties of the Kronecker delta δ_{ij} and Dirac delta $\delta(t)$ to obtain

$$\frac{dn_i}{dt} + \Lambda_i n_i = \sum_{\mu} \lambda_{i\mu} e^{-\Lambda_\mu t} * [\Lambda_\mu \delta(t) + \delta'(t)] * n_\mu(t). \quad (23)$$

Note that

$$e^{-\Lambda_\mu t} * [\Lambda_\mu \delta(t) + \delta'(t)]$$
$$= \Lambda_\mu \int_0^t d\tau e^{-\Lambda_\mu (t-\tau)} \delta(\tau) + \int_0^t d\tau e^{-\Lambda_\mu (t-\tau)} \delta'(\tau)$$
$$= \delta(t),$$

where the integration of the convolution with $\delta'(t)$ is performed using integration by parts. Inserting this result into Eq. (23) yields the rate equation [36]

$$\frac{dn_i}{dt} = \sum_j \lambda_{ij} n_j(t) - \Lambda_i n_i(t), \quad (24)$$

which is driven by the combinatorial Laplacian $L_{ij} = \lambda_{ij} - \Lambda_i \delta_{ij}$ of a weighted network defined by the adjacency matrix λ with components λ_{ij}. Expression (24) thus shows that a random walk on the dynamical graph driven by Eq. (17) is equivalent to a Poisson continuous-time random walk on a static network, which is constructed in the usual manner by counting the number of times edges appear between each pair of nodes. In other words, the rate is equal to the number of observed appearances of an edge divided by the duration of an observation. (In the Poisson case, each observation has the same duration.)

III. STEADY-STATE SOLUTIONS

We expect the walker distribution to settle into a unique steady-state solution as $t \to \infty$ if any node can be reached from any other node. By the so-called final value theorem [37], the steady-state walker density p is

$$p = \lim_{t \to \infty} n(t) = \lim_{s \to 0} s \hat{n}(s).$$

The final value theorem requires that $\hat{n}(s)$ not have any poles in the right half of the complex s plane or on the imaginary axis (except possibly at the origin). As we show later, $s\hat{n}(s)$ has a pole at $s = 0$, and only this pole contributes to the steady-state solution [37].

From Eq. (12), one obtains

$$p = \lim_{s \to 0} (I - \hat{D}_T(s))(I - \hat{T}(s))^{-1} n(0)$$
$$= \mathbb{M} n(0),$$

where the matrix

$$\mathbb{M} \equiv \lim_{s \to 0} (I - \hat{D}_T(s))(I - \hat{T}(s))^{-1}$$

maps the initial state to the final state. In the limit $s \to 0$, one can expand the exponential in the definition of the Laplace transform to first order:

$$[\hat{D}_T(s)]_{ij} = \int_0^\infty (1 - st) T_j(t) \delta_{ij} dt + O(s^2)$$
$$= (1 - s\langle t_j \rangle) \delta_{ij} + O(s^2)$$
$$= (I - s D_{\langle t \rangle})_{ij} + O(s^2),$$

where the resting time $\langle t_j \rangle = \int_0^\infty t T_j(t) dt$ is the mean time spent on node j and we have defined the diagonal matrix $[D_{\langle t \rangle}]_{ij} \equiv \langle t_j \rangle \delta_{ij}$. One can also use the approximation

$$\hat{T}_{ij} = \int_0^\infty [1 - st + O(s^2)] T_{ij}(t) dt$$
$$= \mathbb{T}_{ij} \left(1 - s \int_0^\infty t \frac{T_{ij}(t)}{\mathbb{T}_{ij}} dt + O(s^2) \right)$$
$$= \mathbb{T}_{ij} [1 - s\langle t_{ij} \rangle + O(s^2)], \quad (25)$$

where $\langle t_{ij} \rangle$ is the mean time before making a step $j \to i$. The *effective transition matrix*

$$\mathbb{T}_{ij} \equiv \int_0^\infty T_{ij}(t) dt \quad (26)$$

gives the probability of making a step $j \to i$ and is a measure of the relative importance of an edge. One can write Eq. (25) in matrix form as

$$\hat{T} = \mathbb{T} - s\mathbb{T} \circ \langle t \rangle + O(s^2),$$

where $\circ$ denotes the Hadamard component-wise product.

The operator $\mathbb{M}$ can be written as

$$\mathbb{M} = \lim_{s \to 0} [s D_{\langle t \rangle} (I - \mathbb{T} - s\mathbb{T} \circ \langle t \rangle)^{-1}] + O(s^2),$$

and we expect it to map any initial condition onto a unique one-dimensional vector if the underlying graph $\mathcal{G}$ consists of a single strongly connected component. The steady-state solution is thus given by the leading eigenvector (i.e., the eigenvector corresponding to the maximum eigenvalue, which is guaranteed to be positive) of the operator $\mathbb{M}$. In practice, it is easier to obtain the least dominant eigenvector (i.e., the eigenvector whose corresponding eigenvalue is the smallest in absolute value) of the inverse

$$\begin{aligned}\mathbb{M}^{-1} &= \lim_{s\to 0}\frac{1}{s}\left[I-\mathbb{T}-s\mathbb{T}\circ\langle t\rangle\right]D_{\langle t\rangle}^{-1}\\ &= \lim_{s\to 0}\left[\frac{1}{s}\left(I-\mathbb{T}\right)D_{\langle t\rangle}^{-1}-\left(\mathbb{T}\circ\langle t\rangle\right)D_{\langle t\rangle}^{-1}\right].\end{aligned}$$

In the limit $s\to 0$, the eigenvectors of $\mathbb{M}^{-1}$ tend to the eigenvectors of the matrix $C\equiv(I-\mathbb{T})D_{\langle t\rangle}^{-1}$ because the second term in the second line of the above equation becomes negligible in comparison to the first term. Thus, finding the least dominant eigenvector of C is equivalent to finding the dominant eigenvector of $\mathbb{M}$ in the limit $s\to 0$. Note that $D_{\langle t\rangle}$ is invertible unless the mean time $\langle t_j\rangle$ spent on some node j is 0. This would imply that any walker that arrives at j immediately makes a step to another node i, which would in turn imply that the labels i and j actually refer to the same node. The matrix $D_{\langle t\rangle}$ is thus always invertible in practice.

The operator $\mathbb{T}$ is a stochastic matrix because its columns are normalized (as we have shown in Sec. II E). In particular, if $\mathcal{G}$ is strongly connected, then $\mathbb{T}$ has a single eigenvector x whose eigenvalue is equal to 1 [35].

This implies that the steady-state walker density p is given by

$$p = D_{\langle t\rangle}x, \tag{27}$$

as it is the least dominant eigenvector of C:

$$\begin{aligned}Cp &= (I-\mathbb{T})D_{\langle t\rangle}^{-1}D_{\langle t\rangle}x\\ &= Ix-\mathbb{T}x = 0.\end{aligned}$$

Given the complexity of the stochastic process and the integrodifferential nature of its associated master equation, it is remarkable that one can write down such an exact analytical expression. This equilibrium solution takes a particularly simple form, as it is calculated from the dominant eigenvector of the combinatorial Laplacian associated with the effective transition matrix $\mathbb{T}$. The time spent on node i is thus given by the expected frequency to arrive on i (which is obtained by the Markov chain associated to $\mathbb{T}$) multiplied by the mean waiting time $\langle t_i\rangle$ spent on i. This solution can be computed easily even for very large graphs, as deriving $\mathbb{T}$ from ψ is straightforward and the leading eigenvector of a large matrix can be obtained through standard, efficient techniques (such as the power method).[2]

It remains to be shown that $s\hat{n}(s)$ has a pole at $s=0$, which would guarantee that the requirements of the final value theorem are satisfied. From Eq. (12), it follows that $\hat{n}(s)$ has poles whenever $I-\hat{T}(s)$ is singular. Using Eq. (25), we find in the limit $s\to 0$ that

$$\begin{aligned}(I-\hat{T}(s))x &= (I-\mathbb{T}-s\mathbb{T}\circ\langle t\rangle)\,x+O(s^2)\\ &= Ix-\mathbb{T}x-s\mathbb{T}\circ\langle t\rangle x+O(s^2)\\ &= -s\mathbb{T}\circ\langle t\rangle x+O(s^2).\end{aligned}$$

Hence, in this limit, x is an eigenvector of $I-\hat{T}(s)$ with eigenvalue of 0. Because $\det(I-\hat{T}(s))$ is equal to the product of eigenvalues, $I-\hat{T}(s)$ becomes singular as $s\to 0$.

IV. POISSON VERSUS NON-POISSON PROCESSES

We now discuss some of the differences arising from the non-Poisson nature of the process versus the Poisson situation that is usually considered. For simplicity, we illustrate these differences using an undirected network, for which $\psi_{ij}=\psi_{ji}$. (Recall that the underlying static network has no edge weights.)

For the Poisson process (17), it is straightforward to show from Eq. (18) that the effective transition matrix $\mathbb{T}$ satisfies

$$\mathbb{T}_{ij} = \frac{\lambda_{ij}}{\sum_{i=1}^{N}\lambda_{ij}}, \tag{28}$$

where λ_{ij} is the rate at which the edge between i and j appears in the network, and $\lambda_{ij}=\lambda_{ji}$ because the network is undirected. As we show in detail in the next section, the stationary solution is a uniform vector, which we expect because it is the dominant eigenvector of the Laplacian matrix in Eq. (24).

The case of a non-Poisson process differs significantly from this idealized scenario in at least three ways. First, $\mathbb{T}$ is no longer in general the transition matrix of an undirected network, even in the symmetric case $\psi_{ij}=\psi_{ji}$ that we consider. Evaluating the stationary solution thus requires one to calculate the dominant eigenvector x of $\mathbb{T}$. Second, there is no reason to expect that the stationary solution p is uniform; indeed, it is not uniform in general. Finally, p is a stationary solution only in the limit $t\to\infty$ and not also for intermediate times, as we used an expansion for small s throughout Sec. III to derive its expression. This behavior originates from the time-dependent nature of the stochastic process, as one can see because of the integral over time in the generalized master equation (16). This has interesting implications. For example, a process starting with the stationary solution p as an initial condition exhibits transient deviations to stationarity before returning to its initial condition as $t\to\infty$. In contrast, if the dynamics on the graph are Poisson, then the steady-state solution is time independent. In other words, once the system has reached its steady-state solution, it will stay there.

To illustrate how the nature of the WTDs affects dynamics, consider the example of a completely connected graph with three nodes. Suppose that the WTDs for the processes occurring on the nodes have different functional types and different characteristic times (see Fig. 2). We compare this non-Poisson case to a Poisson process with the same mean rates. The rate matrix is

$$\lambda = \begin{pmatrix}0 & 1 & 2\\ 1 & 0 & 3\\ 2 & 3 & 0\end{pmatrix}.$$

[2]Note that if $\mathcal{G}$ is composed of k strongly connected components, then there are k different eigenvectors with unit eigenvalues. This would then lead to k distinct steady-state solutions rather than the unique one in the strongly connected case.

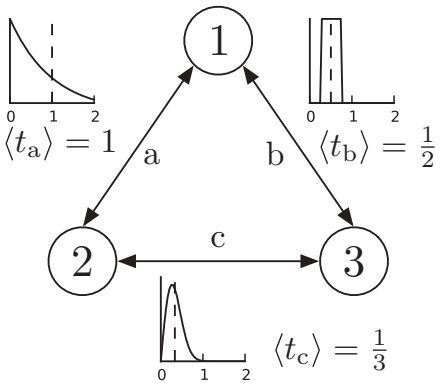

FIG. 2. An undirected network with $N = 3$ nodes and no self-loops. The waiting-time distributions for the edges a, b, and c are exponential, uniform, and Rayleigh, respectively. We denote the corresponding means of these distributions by $\langle t_a \rangle$, $\langle t_b \rangle$, and $\langle t_c \rangle$, respectively. We show the mean of each distribution using a vertical dashed line.

We plot the temporal evolution of the walker densities in Fig. 3 to illustrate the differences between the two processes. We obtain the walker densities from numerical simulations of the random walks with all walkers located initially at node 1. (See the appendix for computational details.) The system relaxes toward a stationary solution in both cases, but the stationary solution clearly depends on the nature of the WTDs, as walkers tend to be underrepresented on node 1 for the non-Poisson dynamics.

In general, the value of the walker density is not sufficient to define the state of the system. The distribution of resting times—that is, the times that a walker spends on a node before making a step—also needs to be specified. Consequently, the walker density temporarily departs from its steady-state value

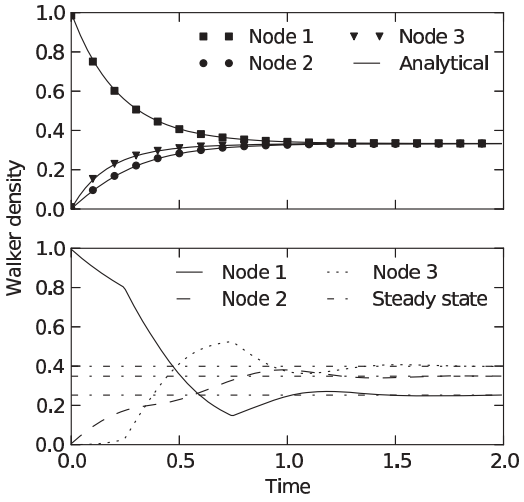

FIG. 3. Random-walker density on each node as a function of time obtained from numerical computations for Poisson (upper panel) and non-Poisson (lower panel) processes. In the former case, we also plot the analytical solution of the rate equation. The error bars are smaller than the widths of the curves used for plotting. For the non-Poisson example, we obtained the steady-state walker density from equation (27). The relaxation towards stationarity exhibits kinks in the dynamics that originate from the noncontinuity of the WTDs.

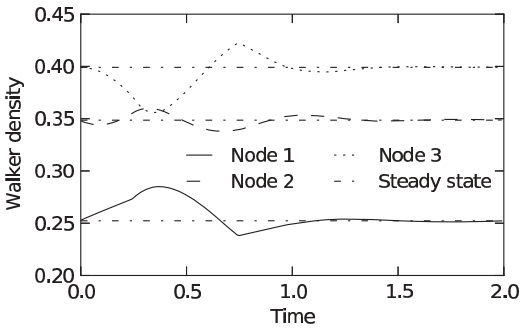

FIG. 4. Random-walker density on each node of the graph illustrated in Fig. 2 as a function of time when the initial condition is the steady-state solution. Due to the time-dependent nature of the dynamics, the system exhibits transient dynamics before returning to its steady-state solution. The error bars are smaller than the widths of the curves used for plotting.

if a process is restarted with its initial walker density equal to the steady-state value (see Fig. 4). However, a Poisson process has no memory—as indicated in Eq. (22), its memory kernel is proportional to a delta function—so its temporal evolution is independent of the distribution of resting times. This can also be understood as a consequence of a unique property of exponential distributions: The probability for an event to occur in a time interval dt is independent of the time since the process started [38]. Setting the walker density to its steady-state value for a Poisson process is thus sufficient for the walker density to remain steady, which is the result expected from the rate equations (24).

V. EXAMPLES: THEORY AND COMPUTATIONS

We consider the steady-state solutions for two different example network topologies (using networks with $N = 10^3$ nodes) to demonstrate the consequences of considering non-Poisson processes. We again use undirected networks as examples.

In general, the steady-state solution of a random walk is given by $p = D_{\langle t \rangle} x$, where x is the dominant eigenvector of the stochastic matrix $\mathbb{T}$. However, for a Poisson process, the steady-state solution is $p_i = \frac{1}{N}$ for all i because the rate of change of all walker densities vanishes according to the rate equations (24):

$$\frac{dn_i}{dt} = \frac{1}{N}\left(\sum_j \lambda_{ij} - \Lambda_i\right) = 0,$$

where we have used $\lambda_{ij} = \lambda_{ji}$. Consequently, the steady-state solution of a Poisson random walk on an undirected network is uniform regardless of the topology of the network and the transition rates associated with the edges.

For non-Poisson random walks, let us consider situations for which the WTDs of all edges are identical. In other words, $\psi_{ij}(t) = \psi(t)A_{ij}$, where A_{ij} is the binary adjacency matrix. Because of this assumption, we can obtain analytical expressions for steady-state solution and thereby demonstrate that the steady-state solutions are nontrivial despite the restrictions placed on the network and the WTDs.

From Eqs. (1), (3), and (26), the effective transition matrix is given by

$$\begin{aligned}\mathbb{T}_{ij} &= -A_{ij}\int_0^\infty \frac{d\chi(t)}{dt}\chi^{d_j-1}(t)dt \\ &= -\frac{1}{d_j}A_{ij}[\chi^{d_j}(t)]_0^\infty \\ &= \frac{1}{d_j}A_{ij},\end{aligned}$$

where $d_j = \sum_{i=1}^N A_{ij}$ is the degree of node j. This is the expected result from symmetry considerations: All WTDs are identical, so the probabilities to make a step to any node are necessarily the same. The dominant eigenvector of $\mathbb{T}_{ij}$ has components $x_j = d_j$ because

$$\begin{aligned}\sum_{j=1}^N \mathbb{T}_{ij}d_j &= \sum_{j=1}^N \frac{1}{d_j}A_{ij}d_j \\ &= \sum_{j=1}^N A_{ij} = 1\times d_i,\end{aligned}$$

where we have used $A_{ij} = A_{ji}$. The mean resting time on node j becomes

$$\begin{aligned}\langle t_j\rangle &= -d_j\int_0^\infty t\frac{d\chi(t)}{dt}\chi^{d_j-1}(t)dt \\ &= \underbrace{-[t\chi^{d_j}(t)]_0^\infty}_{=0} + \int_0^\infty \chi^{d_j}dt.\end{aligned}$$

Consequently, the steady-state solution for a random walk on an undirected network with identical WTDs is

$$p_j = \mathcal{N}d_j\int_0^\infty \chi^{d_j}(t)dt, \tag{29}$$

where $\mathcal{N}$ is a normalization constant. Equation (29) shows that the probability of finding a walker on a node at stationarity only depends on local information (namely, on its degree and the shape of the WTD), which implies that any node with a certain degree must have the same stationary solution. This property arises because the underlying network is undirected and the WTDs are identical—that is, because $\psi_{ij}(t) = \psi(t)$ for all i and j. As we show below, the degree d_j can either increase or decrease the density of walkers p_j on node j at stationarity, depending on $\chi(t)$ and thus on the shape of the WTD.

These results are consistent with the claim that the steady-state solution of a Poisson random walk on an undirected network is uniform. In particular, the mean resting time is

$$\begin{aligned}\langle t_j\rangle_{\text{Poisson}} &= d_j\int_0^\infty [1-(1-e^{-\lambda t})]^{d_j}dt \\ &= \frac{1}{d_j\lambda},\end{aligned}$$

where λ denotes the scalar rate parameter of a Poisson process. The associated steady-state solution is uniform:

$$p_j = \mathcal{N}d_j\frac{1}{d_j\lambda} = \frac{\mathcal{N}}{\lambda}, \quad j\in\{1,\ldots,N\}.$$

Unlike in the Poisson case, the mean resting time $\langle t_j\rangle$ does not in general scale as the inverse of node degree. Consider γ-distributed waiting times with mean μ and standard deviation σ. That is,

$$\psi(t;\mu,\sigma) = \frac{\left(\frac{t\mu}{\sigma^2}\right)^{\mu^2/\sigma^2-1}\exp\left(-\frac{t\mu}{\sigma^2}\right)}{\frac{\sigma^2}{\mu}\Gamma\left(\frac{\mu^2}{\sigma^2}\right)}.$$

When $\sigma/\mu = 1$, the waiting times are exponentially distributed. Hence, we can continuously deform the distribution from an exponential distribution by changing the standard deviation σ while keeping the mean fixed at $\mu = 1$.

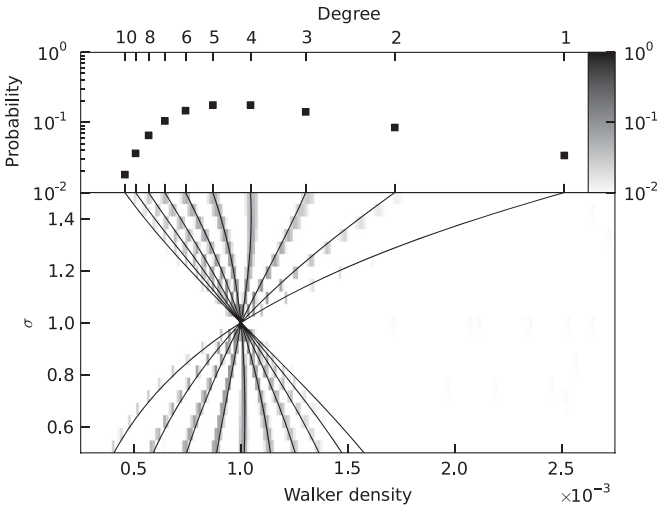

FIG. 5. Distributions of steady-state random walker densities on Erdős-Rényi networks with identical γ-distributed WTDs. The lower panel shows the distinct walker densities associated with a given node degree for a range of standard deviations. We show the results for numerical computations as a density plot in logarithmic coordinates, and we show our analytical results using solid curves. The blurring of the density plot arises from the finite number of simulations. The upper panel shows the degree distribution and the grayscale map for the density plot.

In Fig. 5, we show steady-state solutions on networks generated by the Erdős-Rényi (ER) random graph model [39] for the parameter range $\sigma \in [0.5, 1.5]$. We consider connected networks with $N = 10^3$ nodes and a connection probability of 5×10^{-3}. For our numerics, we generated 10^3 networks and found the steady-state solution by averaging solutions obtained by Eq. (27). We also determined the steady-state solution analytically using Eq. (29) combined with the degree distribution of Erdős-Rényi networks. In Fig. 6, we proceed in the same way for networks generated using a Barabási-Albert (BA) model [40] in which we have connected each new node to three existing nodes.

The computations for both ER and BA networks confirm our theoretical prediction: The behavior is qualitatively different from that expected for Poisson processes even though the mean rates of making steps along all edges are identical. Simulations show that walkers tend to accumulate on low (respectively, high) degree nodes for $\sigma > 1$ (respectively, $\sigma < 1$). In other words, $p_i > p_j$ when $d_i < d_j$ for $\sigma > 1$, whereas $p_i < p_j$ when $d_i < d_j$ for $\sigma < 1$.

VI. DISCUSSION

The overwhelming majority of research that considers dynamics on networks implicitly includes the assumption

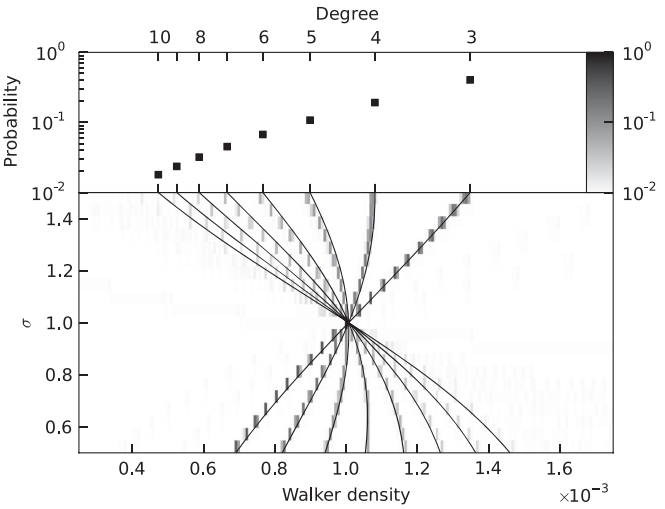

FIG. 6. This figure is the same as Fig. 5, except that we use Barabási-Albert networks instead of ER networks. Note that the smallest degree is 3 because each new node is connected to three existing nodes.

of underlying Poisson processes. For instance, this is the case when one builds an aggregated network from empirical data and assigns only a single number (i.e., a weight) to edges to summarize their dynamics. In that framework, edge weight is understood as a rate of interaction between nodes, so such a choice would imply that events occur in an uncorrelated fashion. The main purpose of the present work is to consider a mathematical framework that goes beyond this oversimplification and thereby propose a compromise between abstract but unrealistic models and data-driven but nonmathematical approaches for studying temporal networks. In the proposed framework, we view temporal networks as sequences of realizations of random networks in which present events depend on past ones. We summarize the temporal and structural organization of a system by a matrix of WTDs that characterizes the activation patterns of edges between nodes. In this paper, we have derived a generalized master equation for a random walk associated with this process, obtained an expression for its stationary solution, used a sample network to highlight the importance of the shape of WTDs, and illustrated our results using Erdős-Rényi and Barabási-Albert networks.

The present paper is a step towards a mathematical description of temporal networks, and it suggests several research directions. An important step is the thorough consideration of empirical data, such as human communication patterns, to help design appropriate WTDs and to study how their shape affects equilibrium solutions. This step is related to the development of network diagnostics that properly take into account the temporal dynamics of complex systems [41–44], whose behavior arises not only from their structural patterns but also from their dynamics. The investigation of complex systems thus requires the development of diagnostics that consider both structure and dynamics [36]. The fact that most existing network diagnostics account only for the presence, weight, and direction of edges and assume that they are present for all time presupposes an underlying Poisson process, which can yield a fundamentally incorrect representation of a system. Indeed, assuming a Poisson waiting time can be as unrealistic as assuming that the topology of a network is organized like an Erdős-Rényi random graph. It is thus crucial to develop network concepts that account for nontrivial temporal dynamics. This includes centrality measures (such PageRank [45]), which measure the importance of network components in various ways, and the components of the steady-state solution vector derived in this paper provide an example of one such diagnostic. Another example is community-detection methods based on the idea that non-Poisson random walkers are trapped for long times in good communities [46,47], though of course there is much more that one can do. Other interesting research directions include the development of a sound mathematical framework for various dynamical processes, such as synchronization or epidemic spreading [27], and the study of random walks with alternative ways to build the matrix of waiting times. For example, the dynamics could be driven by the normalized Laplacian in the Poisson limit.

ACKNOWLEDGMENTS

We thank T. Carletti, J.-C. Delvenne, P. J. Mucha, M. Rosvall, and J. Saramäki for fruitful discussions.

APPENDIX: NUMERICAL SIMULATION

We implemented our numerical simulations using PYTHON. The approach in this paper requires computing the probability of finding a walker on a certain node. To approximate this numerically, we simulate 10^6 random walks for each scenario and average over the realizations of the walk in order to estimate the walker density numerically.

1. Generating trajectories

We generate the trajectory of a walker by making steps on a graph $\mathcal{G}$ until the maximum simulation time $t_{\max}$ is reached. See algorithm 1.

Algorithm 1 Generation of the trajectory of a random walker on a graph $\mathcal{G}$ starting at an origin node.

```
function TRAJECTORY(G, origin, t_max)
    t ← 0
    current ← origin
    steps ← {(t, current)}
    while t < t_max do
        δ ← ∞
        for p_{i,current} ∈ G do
            δ' ← random sample following p_{i,current}
            if δ' < δ then
                successor ← i
                δ ← δ'
            end if
        end for
        current ← successor
        t ← t + δ
        add (t, current) to steps
    end while
    return steps
end function
```

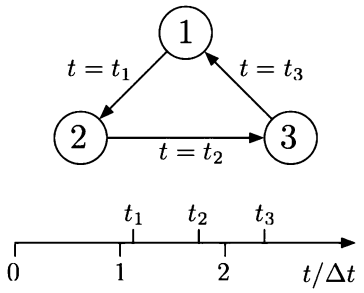

FIG. 7. A random walker makes three steps on a graph of three nodes at irregular intervals.

2. Averaging over different realizations

Each of the 10^6 different realizations includes steps at irregular times. We consider a set of k finite intervals of uniform width $\Delta t = 0.01$ such that $k\Delta t = t_{\max}$. The probability of finding a random walker on node j during a certain interval is then given by the mean over all realizations of the fraction of the time spent on j during this interval. Consider a single realization of a random walk on a graph of three nodes (see Fig. 7). In Table I, we give the fractions of time spent on each of the nodes in the contribution to the average.

TABLE I. Fractions of time spent on each node in Fig. 7 during the first three intervals.

Interval	Node 1	Node 2	Node 3
1	1	0	0
2	0.125	0.625	0.25
3	0.625	0	0.375

[1] M. E. J. Newman, *Networks: An Introduction* (Oxford University Press, Oxford, 2010).
[2] R. Durrett, Proc. Natl. Acad. Sci. USA **107**, 4491 (2010).
[3] S. Boccaletti, V. Latora, Y. Moreno, M. Chavez, and D.-U. Hwang, Phys. Rep. **424**, 175 (2006).
[4] P. Holme and J. Saramäki, arXiv:1108.1780 [Phys. Rep. (to be published)].
[5] D. Kempe, J. Kleinberg, and A. Kumar, J. Comput. Syst. Sci. **64**, 820 (2002).
[6] A. Ferreira, in *Proceedings of 4émes Rencontres Francophones sur les Aspects Algorithmiques des Télécommunications (ALGO-TEL2002)* (Méze, France, 2002), pp. 155–161.
[7] J. L. Iribarren and E. Moro, Phys. Rev. Lett. **103**, 038702 (2009).
[8] J. Tang, S. Scellato, M. Musolesi, C. Mascolo, and V. Latora, Phys. Rev. E **81**, 055101(R) (2010).
[9] L. E. C. Rocha, F. Liljeros, and P. Holme, Proc. Natl. Acad. Sci. USA **107**, 5706 (2010).
[10] M. Karsai, M. Kivelä, R. K. Pan, K. Kaski, J. Kertész, A.-L. Barabási, and J. Saramäki, Phys. Rev. E **83**, 025102(R) (2011).
[11] T. Takaguchi and N. Masuda, Phys. Rev. E **84**, 036115 (2011).
[12] J. Fernández-Gracia, V. M. Eguíluz, and M. San Miguel, Phys. Rev. E **84**, 015103 (2011).
[13] A. Vazquez, B. Rácz, A. Lukács, and A.-L. Barabási, Phys. Rev. Lett. **98**, 158702 (2007).
[14] L. Sabatelli, S. Keating, J. Dudley, and P. Richmond, Eur. Phys. J. B **27**, 273 (2002).
[15] J. Kleinberg, Data Mining Knowledge Disc. **7**, 373 (2003).
[16] J.-P. Eckmann, E. Moses, and D. Sergi, Proc. Natl. Acad. Sci. USA **101**, 14333 (2004).
[17] A.-L. Barabási, Nature (London) **435**, 207 (2005).
[18] R. D. Malmgren, D. B. Stouffer, A. E. Motter, and L. A. N. Amaral, Proc. Natl. Acad. Sci. USA **105**, 18153 (2008).
[19] J. G. Oliveira and A.-L. Barabási, Nature (London) **437**, 1251 (2005).
[20] R. Kumar, J. Novak, P. Raghavan, and A. Tomkins, in *Proceedings of the 12th International Conference on World Wide Web (WWW)* (Association for Computing Machinery, New York, 2003), pp. 568–576.
[21] R. Lambiotte, M. Ausloos, and M. Thelwall, J. Informetrics **1**, 277 (2007).
[22] L. Isella, C. Cattuto, W. Van den Broeck, J. Stehlé, A. Barrat, and J.-F. Pinton, J. Theor. Biol. **271**, 166 (2011).
[23] M. Begeurisse Díaz, M. A. Porter, and J.-P. Onnela, Chaos **20**, 043101 (2010).
[24] P. Caley, N. G. Becker, and D. J. Philp, PLoS ONE **2**, e143 (2007).
[25] N. E. Friedkin and E. C. Johnson, *Social Influence Network Theory* (Cambridge University Press, Cambridge, 2011).
[26] H. W. Hethcote and D. W. Tudor, J. Math. Biol. **9**, 37 (1980).
[27] B. Karrer and M. E. J. Newman, Phys. Rev. E **82**, 016101 (2010).
[28] E. W. Montroll and G. H. Weiss, J. Math. Phys. **6**, 167 (1965).
[29] J. Klafter and I. M. Sokolov, Phys. World **18**, 29 (2005).
[30] V. M. Kenkre, J. D. Andersen, D. H. Dunlap, and C. B. Duke, Phys. Rev. Lett. **62**, 1165 (1989).
[31] P. P. G. Dyke, *An Introduction to Laplace Transforms and Fourier Series* (Springer, Berlin, Germany, 1999).
[32] H. Scher and M. Lax, Phys. Rev. B **7**, 4491 (1973).
[33] R. Balescu, *Statistical Dynamics* (Imperial College Press, London, UK, 1997).
[34] M. R. Spiegel, *Laplace Transforms* (McGraw-Hill, New York, 1992).
[35] W. J. Stewart, *Probability, Markov Chains, Queues, and Simulation: The Mathematical Basis of Performance Modeling* (Princeton University Press, Princeton, NJ, 2009).
[36] R. Lambiotte, R. Sinatra, J.-C. Delvenne, T. S. Evans, M. Barahona, and V. Latora, Phys. Rev. E **84**, 017102 (2011).
[37] J. C. Jaeger and G. Newstead, *An Introduction to the Laplace Transformation with Engineering Applications* (Methuen, London, UK, 1969).
[38] P. Hoel, S. Port, and C. Stone, *Introduction to Probability Theory* (Houghton Mifflin, Boston, MA, 1971).
[39] P. Erdős and A. Rényi, *On the Evolution of Random Graphs* (Akad. Kiadó, Budapest, Hungary, 1960).
[40] A. Barabási and R. Albert, Science **286**, 509 (1999).
[41] J. Tang, M. Musolesi, C. Mascolo, and V. Latora, in *Proceedings of the Second ACM SIGCOMM Workshop on Online Social*

Networks (WOSN'09) (Association for Computing Machinery, New York, 2009), pp. 118–124.

[42] P. Grindrod, D. J. Higham, M. C. Parsons, and E. Estrada, Phys. Rev. E **83**, 046120 (2011).

[43] R. K. Pan and J. Saramäki, Phys. Rev. E **84**, 016105 (2011).

[44] P. J. Mucha, T. Richardson, K. Macon, M. A. Porter, and J.-P. Onnela, Science **328**, 876 (2010).

[45] S. Brin and L. Page, in *Proceedings of the Seventh International Conference on World Wide Web (WWW)* (Association for Computing Machinery, New York, 1998), pp. 107–117.

[46] M. Rosvall and C. T. Bergstrom, Proc. Natl. Acad. Sci. USA **105**, 1118 (2008).

[47] J.-C. Delvenne, S. Yaliraki, and M. Barahona, Proc. Natl. Acad. Sci. USA **107**, 12755 (2010).